

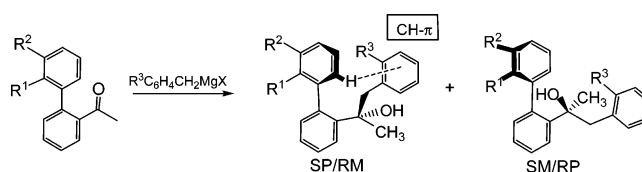
## Stereodynamics and Edge-to-Face CH- $\pi$ Aromatic Interactions in *o*-Phenethyl-Substituted Biaryls

W. Brian Jennings,<sup>\*,†</sup> Brid M. Farrell,<sup>†,§</sup> and John F. Malone<sup>\*,‡</sup>

Department of Chemistry and Analytical & Biological Chemistry Research Facility, University College Cork, Cork, Ireland, and School of Chemistry and Chemical Engineering, The Queen's University of Belfast, Belfast BT9 5AG, Northern Ireland

brianj@ucc.ie

Received October 5, 2005



As part of a search for systems that exhibit intramolecular aromatic edge-to-face interactions, a series of four biaryl compounds containing a phenethyl side chain were prepared. These compounds exist as a slowly interconverting mixture of two atropisomers due to steric hindrance to rotation about the biaryl bond. The more thermodynamically stable isomer exhibits an abnormal shielding of an *ortho*-proton in solution indicative of an edge-to-face CH- $\pi$  interaction with the terminal phenyl ring on the side chain. This tilted-T type of geometry was observed in the X-ray crystal structure of one of the compounds. The edge-to-face conformation in solution is estimated by variable temperature NMR studies to be energetically favored by ca. 1.6 kcal mol<sup>-1</sup> but entropically disfavored by ca. 5.0 cal K<sup>-1</sup> mol<sup>-1</sup>.

### Introduction

Edge-to-face orientations between aromatic rings were initially observed almost 50 years ago in the herringbone structure of crystalline benzene.<sup>1</sup> However the more general significance of these relatively weak edge-to-face CH- $\pi$  aromatic interactions did not become evident until 1985 when Burley and Petsko, and Singh and Thornton presented evidence that they played a significant role in protein structure.<sup>2</sup> Edge-to-face aromatic interactions can also be important in such diverse areas as crystal packing and crystal engineering,<sup>3,4</sup> supramolecular assemblies and host-guest binding,<sup>5</sup> drug receptor interactions,<sup>6</sup> and other areas of molecular recognition.<sup>7</sup> Examples have emerged where intramolecular edge-to-face interactions have a considerable role in determining the conformation of flexible organic molecules in solution and in the crystalline state. Molecular orbital calculations and evidence from some crystal structures indicate that the geometry of edge-to-face interactions can be classified

into three categories: T-shaped, tilted-T (subdivided into face and edge tilted), and offset parallel.<sup>8</sup> All of the above arrangements are believed to be attractive by ca. 1–2 kcal mol<sup>-1</sup>, but more examples are needed in order to provide additional information.

Following previous observations of edge-to-face aromatic interactions in imino systems,<sup>9</sup> we now report the occurrence of these interesting interactions in twisted biphenyl systems containing an *ortho*  $\alpha$ -hydroxyphenethyl substituent.

### Results and Discussion

**Synthesis and Stereodynamics.** Synthesis of the hindered target compounds **3–6** was achieved in just four steps from

<sup>†</sup> University College Cork.

<sup>‡</sup> The Queen's University of Belfast.

<sup>§</sup> Present address: GlaxoSmithKline Manufacturing Ltd., Currabinny, Carrigaline, Co. Cork, Ireland.

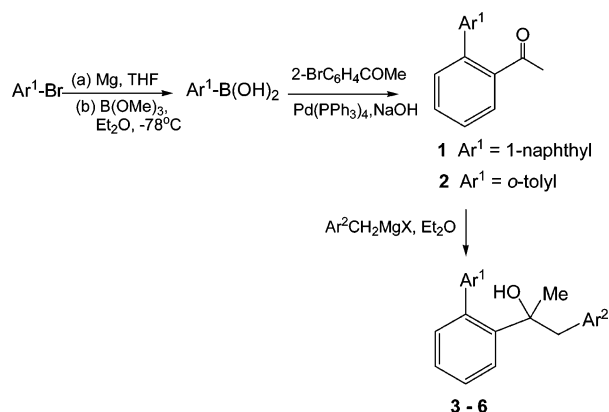
(1) Cox, E. G.; Cruickshank, D. W. J.; Smith, J. A. S. *Proc. R. Soc. London* **1958**, *247*, 1–21.

(2) (a) Burley, S. K.; Petsko, G. A. *Science* **1985**, *229*, 23–28. (b) Singh, J.; Thornton, J. M. *FEBS Lett.* **1985**, *191*, 1–6. (c) Burley, S.K.; Petsko, G. A. *Adv. Protein Chem.* **1988**, *39*, 125–189.

(3) For a review see: Nishio, M. *CrystEngComm* **2004**, *6*, 130–158.

(4) Some recent examples: (a) Brayshaw, P. A.; Hall, A. K.; Harrison, W. T. A.; Harrowfield, J. M.; Pearce, D.; Shand, T. M.; Skelton, B. W.; Whitaker, C. R.; White, A. H. *Eur. J. Inorg. Chem.* **2005**, *6*, 1127–1141. (b) Oh, M.; Stern, C. L.; Mirkin, C. A. *Inorg. Chem.* **2005**, *44*, 2647–2653. (c) Abboud, K.; Harrowfield, J. M.; James, B. D.; Skelton, B. W.; White, A. H. *Inorg. Chim. Acta* **2005**, *358*, 1293–1297. (d) Soudi, A. A.; Marandi, F.; Ramazani, A.; Ahmadi, E.; Morsali, A. C. R. *Chim.* **2005**, *8*, 157–168. (e) Reger, D. L.; Semeniuc, R. F.; Smith, M. D. *Cryst. Growth Des.* **2005**, *5*, 1181–1190. (f) Harrowfield, J.; Matt, D. *J. Inclusion Phenom. Macrocyclic Chem.* **2004**, *50*, 133–150. (g) Emseis, P.; Hibbs, D. E.; Leverett, P.; Reddy, N.; Williams, P. A. *Inorg. Chim. Acta* **2004**, *357*, 3251–3263. (h) Xu, W.; Lu, Y. X.; Liu, C. M.; Guo, P.; Lan, B. J.; Zhou, H. *Acta Crystallogr., Sect. E: Struct. Rep. Online* **2004**, *60*, 1049–1050. (i) Yang, J. S.; Liu, C. P.; Lin, B. C.; Tu, C. W.; Lee, G. H. *J. Org. Chem.* **2002**, *67*, 7343–7354.

## SCHEME 1. Synthetic Route

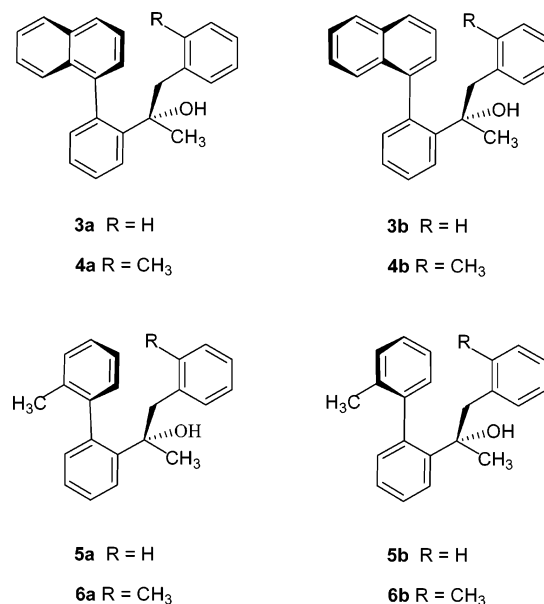


commercially available 2-bromonaphthalene or 2-bromotoluene (Scheme 1). These aryl bromides were converted to the corresponding boronic acids via the Grignard reagents. Aryl coupling to 2-bromoacetophenone was achieved in good yield (80%) via a Suzuki coupling reaction to afford the biaryl ketones **1** and **2**. Addition of benzyl- or 2-methylbenzyl-magnesium bromide in ether gave the target biaryl carbinols **3–6** in good yield (60–90%) as a mixture of two diastereomers as shown by NMR analysis.

The diastereomers are atropisomers arising from slow rotation on the NMR time-scale around the biaryl bond. This generates a chiral axis with *M* or *P* configuration, which in combination with the stereogenic carbinol center gives two racemic diastereomers *RM/SP* and *RP/SM* (Chart 1). In the case of the naphthyl compounds **3** and **4** the diastereomers were separated by flash column chromatography on silica gel. The diastereomers of the *o*-tolyl compounds **5** and **6** failed to separate completely, but pure samples were obtained by recrystallizing partially resolved chromatography fractions.

In each of the compounds the more quickly eluted isomer (**3a–6a**) was the minor component of the reaction mixture (25–33%). The isomer distribution was found to be under kinetic control as the ratio was observed to change markedly on heating the samples to 90–120 °C in toluene-*d*<sub>8</sub> or 1,1,2,2-tetrachloroethane-*d*<sub>2</sub>. The initial (kinetic) and final equilibrium (thermodynamic) isomer ratios are given in Table 1 as determined by integration of the respective signals in the <sup>1</sup>H NMR spectra. Interestingly, the more quickly eluted minor diastereomer is actually the thermodynamically preferred isomer in each case accounting for 60–68% of the equilibrium mixture (Table 1). Neither the initial kinetic nor the equilibrium isomer distributions

## CHART 1. Structures and Relative Stereochemistry

TABLE 1. Atropisomer Ratios under Kinetic and Thermodynamic Control<sup>a</sup>

compd	kinetic ratio a:b	thermodynamic ratio a:b
<b>3</b>	25:75	68:32 <sup>b</sup>
<b>4</b>	28:72	60:40 <sup>c</sup>
<b>5</b>	27:73	64:36 <sup>d</sup>
<b>6</b>	33:67	62:38 <sup>d</sup>

<sup>a</sup> Measured by integration of <sup>1</sup>H NMR signals. <sup>b</sup> Measured at 83 °C in 1,1,2,2-tetrachloroethane-*d*<sub>2</sub> after equilibration. <sup>c</sup> Measured at 110 °C in 1,1,2,2-tetrachloroethane-*d*<sub>2</sub> after equilibration. <sup>d</sup> Measured at 61 °C in chloroform-*d* after equilibration.

TABLE 2. Kinetic Data for Atropisomerization

compd	<i>T</i> (°C)	<i>k</i> <sub>a→b</sub> <sup>a</sup> (s <sup>-1</sup> )	<i>k</i> <sub>b→a</sub> <sup>a</sup> (s <sup>-1</sup> )	Δ <i>G</i> <sup>‡</sup> <sub>a→b</sub> <sup>b</sup> (kcal mol <sup>-1</sup> )	Δ <i>G</i> <sup>‡</sup> <sub>b→a</sub> <sup>b</sup> (kcal mol <sup>-1</sup> )
<b>3b</b>	83 <sup>c</sup>	2.25 × 10 <sup>-6</sup>	4.75 × 10 <sup>-6</sup>	30.2	29.7
<b>5a</b>	61 <sup>d</sup>	1.07 × 10 <sup>-5</sup>	1.93 × 10 <sup>-5</sup>	27.2	26.9

<sup>a</sup> Estimated precision ± 10%. <sup>b</sup> Estimated precision ± 0.1 kcal mol<sup>-1</sup>. <sup>c</sup> Solvent 1,1,2,2-tetrachloroethane-*d*<sub>2</sub>. <sup>d</sup> Solvent chloroform-*d*.

vary much with structure on changing the Ar<sup>1</sup> group from 1-naphthyl (**3** and **4**) to *o*-tolyl (**5** and **6**) or Ar<sup>2</sup> from phenyl (**3** and **5**) to *o*-tolyl (**4** and **6**). Raising the temperature facilitates interconversion of the isomers by rotation about the hindered central biaryl bond.

Compounds **3b** and **5a** were selected for a kinetic study of the atropisomerization. The process was followed by <sup>1</sup>H NMR using the change in relative intensity of the methyl signals. The kinetics followed the standard pattern for a reversible first-order approach to equilibrium and the results are given in Table 2. The free energy of activation is about 3 kcal mol<sup>-1</sup> lower for compound **5**. The interconversion involves passage of the Ar<sup>1</sup> ring through the plane of the directly attached *ortho*-substituted phenyl ring. The least congested transition state will involve the 1-naphthyl group in **3**, or the *o*-tolyl group in **5**, passing the *ortho*-hydrogen atom of the second ring. Clearly it is sterically easier for an *o*-tolyl group to adopt the coplanar biaryl geometry than it is for a 1-naphthyl group. Literature reports on other systems also indicate that rotational barriers involving a 1-naphthyl group are 2–3 kcal mol<sup>-1</sup> larger than those involving

(5) (a) Reger, D. L.; Watson R. P.; Smith, M. D.; Pellechia, P. J. *Organometallics* **2005**, *24*, 1544–1555. (b) Lukyanenko, N. G.; Kirichenko, T. I.; Lyapunov, A. Y.; Mazepa, A. V.; Simonov, Y. A.; Fonari, M. S.; Botoshansky, M. M. *Chem.—Eur. J.* **2004**, *11*, 262–270. (c) Leonard, M. S.; Carroll, P. J.; Joulie, M. M. *J. Org. Chem.* **2004**, *69*, 2526–2531. (d) Balog, M.; Grosu, I.; Ple, G.; Ramondenc, Y.; Condamine, E.; Varga, R. A. *J. Org. Chem.* **2004**, *69*, 1337–1345.

(6) (a) Sukalovic, V.; Andric, D.; Roglic, G.; Kostic-Rajacic, S.; Schratzenholz, A.; Soskic, V. *Eur. J. Med. Chem.* **2005**, *40*, 481–493. (b) Sukalovic, V.; Zlatovic, M.; Andric, D.; Roglic, G.; Kostic-Rajacic, S.; Soskic, V. *Arzneim.—Forsch.* **2005**, *55*, 145–152. (c) Fattori, D. *Drug Discovery Today* **2004**, *9*, 229–238.

(7) Shu, L. H.; Shi, Y. *Tetrahedron Lett.* **2004**, *45*, 8115–8117.

(8) For a review, see: Jennings, W. B.; Farrell, B. M.; Malone, J. F. *Acc. Chem. Res.* **2001**, *34*, 885–894.

(9) (a) Boyd, D. R.; Evans, T. A.; Jennings, W. B.; Malone, J. F.; O'Sullivan, W. O.; Smith, A. *Chem. Commun.* **1996**, 2269–2270. (b) Hamor, T. A.; Jennings, W. B.; Proctor, L. D.; Tolley, M. S.; Boyd, D. R.; Mullan, T. J. *Chem. Soc., Perkins Trans. 2* **1990**, 25–30.

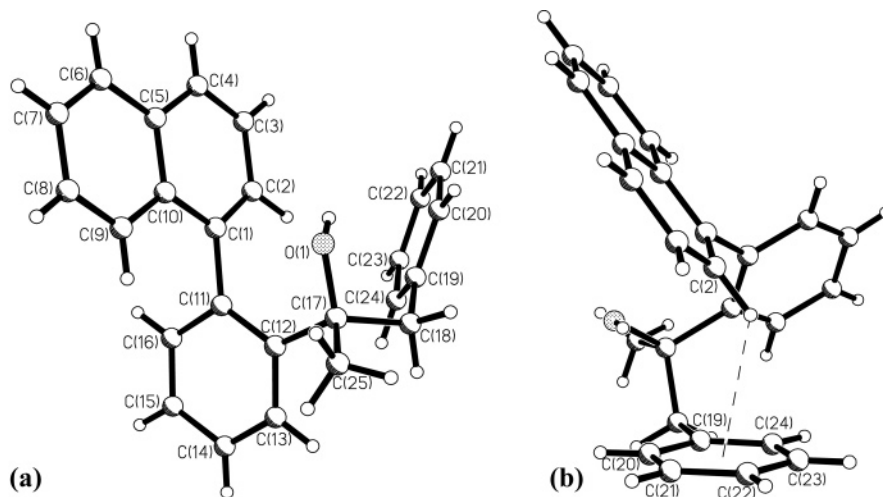


FIGURE 1. X-ray structure of **3a** showing (a) atom numbering and (b) edge-to-face interaction.

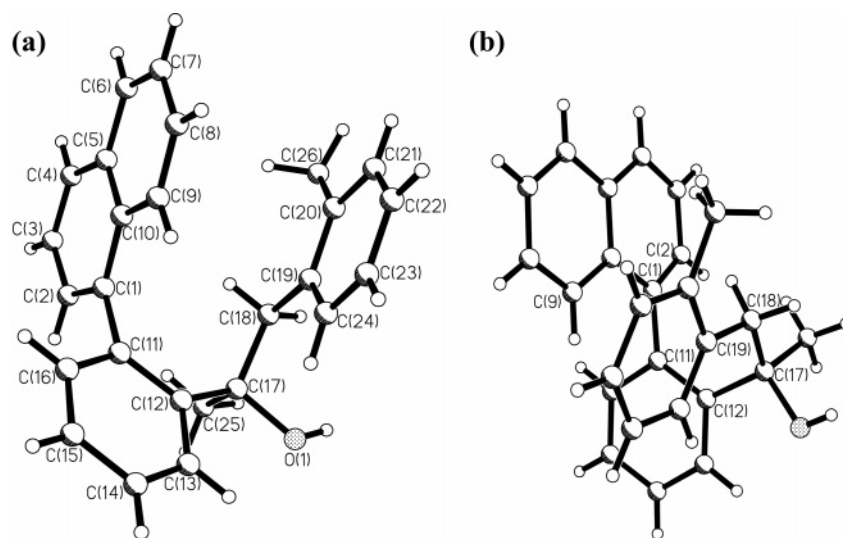


FIGURE 2. Two views of the X-ray structure of **4a**, with atom numbering.

an *o*-tolyl group.<sup>10</sup> In each case the thermodynamically preferred atropisomer **a** showed in the <sup>1</sup>H NMR spectrum an aromatic doublet signal at abnormally high field:  $\delta$  6.19 (**3a**), 6.44 (**4a**), 5.90 (**5a**), and 6.07 (**6a**). The kinetic atropisomers **3b–6b** did not show this upfield aromatic signal. The upfield doublet signal of the **a** isomers integrated for one proton (relative to the corresponding methyl signals) and showed evidence of additional *meta* coupling. This signal is assigned to the proton H2 on the Ar<sup>1</sup> ring *ortho* to the biphenyl bond. This assignment was confirmed by 500 MHz HMBC, HMQC, COSY and TOCSY 2D NMR spectra of **3a**, **4a**, **5a**, and **6a**. The upfield shift of aromatic protons in rings devoid of strong electron donating substituents is characteristic of a proton experiencing ring current shielding due to an edge-to-face interaction with the face of a neighboring aromatic ring. The only feasible source of the shielding in the present compounds is the terminal Ar<sup>2</sup> ring on the side chain.

**X-ray Crystal Structures.** To investigate the possibility of an edge-to-face interaction in the solid state, the two minor

component naphthyl compounds, **3a** and **4a**, which provided suitable crystals, were subjected to single-crystal X-ray analysis. In both compounds all hydrogen atoms were located from difference Fourier syntheses but were included in the final calculations at positions calculated from the geometries of the molecules. For the hydrogen atoms being examined for possible interaction with a second aromatic ring in an edge-to-face contact, the hydrogen was positioned to give a C–H bond length of 1.083 Å, the standard value obtained from neutron diffraction determination of the position of the hydrogen nucleus, and used in earlier studies as a normalized distance.<sup>8</sup>

Both **3a** and **4a** have configuration RM/SP (shown as RM in Figures 1 and 2). Since all four **a** isomers show similar upfield aromatic signals in their <sup>1</sup>H NMR spectra and are thermodynamically more stable, it can be reasonably assumed that **5a** and **6a** also have the RM/SP configuration. The atom numberings for **3a** and **4a**, respectively, are shown in Figures 1 and 2.

The conformation adopted by **3a** in the crystalline state is classified as a face-tilted T-geometry.<sup>8</sup> Thus the ortho hydrogen, H2, of the naphthyl group is located above the plane of the terminal Ar<sup>2</sup> phenyl ring (C19–C24; Figure 1b). The H to ring-

(10) (a) Boyd, D. R.; Al-Showiman, S.; Jennings, W. B. *J. Org. Chem.* **1978**, *43*, 3335–3339. (b) Jennings, W. B.; Kochanewycz, M. J.; Lunazzi, L. *J. Chem. Soc., Perkin Trans. 2* **1997**, 2271–2273.

**TABLE 3.** Torsion Angles (deg)

compd	C10–C1– C11–C12	C11–C12– C17–C18	C12–C17– C18–C19	C17–C18– C19–C20
<b>3a</b>	–102	–114	+67	+87
<b>4a</b>	–100	+49	+56	+185

**TABLE 4.** Estimated Enthalpy ( $\Delta H^\circ$ ) and Entropy ( $\Delta S^\circ$ ) Changes for the Proposed Closed (I)  $\rightleftharpoons$  Open (II) Conformational Equilibrium

compd	temp range (°C)	$\delta_I$	$\delta_{II}$	$\Delta H^\circ$ <sup>a</sup> (kcal mol <sup>-1</sup> )	$\Delta S^\circ$ <sup>a</sup> (cal mol <sup>-1</sup> K <sup>-1</sup> )	$\Delta G^\circ$ <sup>b</sup> (kcal mol <sup>-1</sup> )
<b>3a</b>	–80 to 20	4.8	7.7	1.5	4.9	0.05
<b>5a</b>	–50 to 20	5.0	7.5	1.7	5.0	0.24

<sup>a</sup> Estimated precision:  $\Delta H^\circ \pm 0.3$  kcal mol<sup>-1</sup>;  $\Delta S^\circ \pm 0.5$  cal mol<sup>-1</sup> K<sup>-1</sup>.  
<sup>b</sup> Measured at 20 °C, precision  $\pm 0.2$  kcal mol<sup>-1</sup>.

centroid distance is 2.64 Å. The perpendicular distance from H2 to the Ar<sup>2</sup> ring is 2.59 Å, and the point of intersection of this perpendicular to the plane is offset by 0.52 Å from the ring centroid. These distances are among the shortest found in previous face-tilted aromatic contacts<sup>8</sup> and represent a substantial edge-to-face interaction. Moreover the dihedral angle of 53° between the interacting aromatic rings is typical of angles found in earlier examples of other systems exhibiting an edge-to-face interaction.<sup>8</sup>

Surprisingly, compound **4a** (Figure 2) adopts a very different conformation in the solid state. Figures 1a and 2b, respectively, show molecules **3a** and **4a** from a similar perspective with respect to the biaryl group. The differences in molecular conformation can be quantified by comparing the torsion angles along the four rotatable bonds between the naphthyl and terminal phenyl groups (Table 3).

Relative to the conformation of **3a**, compound **4a** shows a 163° rotation about the C12–C17 bond and a 102° rotation about C18–C19. Thus the naphthyl *ortho*-proton, H2, is removed from the vicinity of the Ar<sup>2</sup> ring (Figure 2b), and the edge-to-face contact of H2 indicated by NMR in solution is absent in the solid state. The closest approach of any aromatic proton in **4a** to a second ring is between the naphthyl *peri* proton (H9) and the terminal tolyl ring. The H9 to tolyl ring-centroid distance, 3.15 Å, is probably beyond an accepted limit for a strong edge-to-face interaction. However, the perpendicular distance, H9 to ring plane, 2.92 Å, with offset 1.18 Å and a very shallow 18° interplanar angle is suggestive of a weak distorted offset-stacked edge-to-face interaction. Possibly crystal packing forces are responsible for the unexpected geometry of compound **4a** in the solid state. Alternatively **4a** may have crystallized in a conformation approximating to the “open” conformer believed to be in rapid equilibrium with the face-tilted T conformation in solution (see Solution Dynamics). Indeed it can be estimated from the small  $\Delta G^\circ$  for this equilibrium (Table 4) that there is ca. 40–50% of at least one alternative conformation present in solution at room temperature, offering an opportunity for the compound to crystallize in this geometry.

**Solution Dynamics.** In solution compounds **3–6** will have rapid conformational mobility about all three single bonds in the phenethyl side chain. Mobility about the biphenyl bond is severely restricted at ambient temperature, leading to the separable atropisomers **a** and **b**. To create the observed marked shielding of the *ortho* A<sup>1</sup> ring proton in compounds **3a**, **4a**, **5a**,

and **6a** there must be a considerable population of a sice chain conformation that places the Ar<sup>2</sup> phenyl or tolyl ring in a face-to-edge orientation with this proton, as observed in the solid-state structure of **3a**. Although the shielding effect on proton H2 in solution is sizable (ca. 1.5 ppm based on a standard aromatic signal position of ca.  $\delta$  7.5), it is less than the shielding predicted for a proton fixed 2.59 Å above the face of the Ar<sup>2</sup> ring (ca. 2.5 ppm using the Johnson–Bovey ring current tables).<sup>11</sup>

We propose that in solution the edge-to-face “closed” conformation is in rapid equilibrium with at least one “open” conformation that does not have a close association between the Ar<sup>2</sup> ring and the *ortho* proton on Ar<sup>1</sup>.<sup>8,9</sup> Hence the actual shift of this proton is a time average of the shifts in the open and closed conformations weighted according to their relative populations.<sup>9</sup> This leads to an observed signal position well upfield of the normal aromatic value of ca.  $\delta$  7.5 but short of the predicted position of ca.  $\delta$  5.0 for an edge-to-face interaction at 2.59 Å. To test this postulate two representative compounds **3a** and **5a** were subjected to a variable-temperature NMR study. The relative conformer populations in a dynamic situation should change with temperature (unless they happen fortuitously to have equal energy and the same entropy). The temperature effect on conformational equilibria is greatest in situations where enthalpic and entropic factors are in opposition, i.e., where the lower energy conformation has the lowest (less favorable) entropy.

On lowering the temperature, the shielded *ortho* doublet signal of the naphthyl compound **3a** steadily moved further upfield from  $\delta$  6.20 at 20 °C to  $\delta$  5.60 at –50 °C in CD<sub>2</sub>Cl<sub>2</sub> solution. To extract the thermodynamic factors determining the conformational equilibrium it is necessary to have an estimate of the shifts of this proton in both the open and closed (edge-to-face) conformations. Initially these values were taken to be  $\delta_{II}$  7.5 as being typical of an aromatic proton *ortho* to an imino group in the absence of any ring current effect and  $\delta_I$  5.0 estimated from the Johnson–Bovey ring current tables for a proton in the closed edge-to-face conformation using the X-ray data for **3a**.<sup>11</sup> However, in the final computer-based analysis both of these estimates were varied slightly to optimize the agreement between calculated and observed chemical shift versus temperature curves (Table 4). The resulting values of  $\Delta H^\circ$  and  $\Delta S^\circ$  were reasonably robust (within 10%) to the precise values of  $\delta_I$  and  $\delta_{II}$  used in the calculation.

It can be seen from the results in Table 4 that the closed edge-to-face conformation (I) has significantly lower enthalpy (by ca. 1.6 kcal mol<sup>-1</sup>) consistent with the supposed attractive nature of this interaction. However, entropic factors strongly favor the open conformation, presumably due to its greater flexibility. A similar trend was previously observed for edge-to-face interactions in imino compounds.<sup>9</sup> It is possible that there is more than one significantly populated open conformation. This would not invalidate the model provided that, as expected, the chemical shift ( $\delta_{II}$ ) of all open conformations lies in the normal aromatic region (ca.  $\delta$  7.5). However significant contributions from more than one open conformation would further raise the entropy due to a contribution from entropy of mixing (RlnN).

(11) The ring current shielding of a proton situated 2.59 Å vertically above the face of a phenyl ring and offset from the center by 0.52 Å (as in the X-ray structure of **3a**) was estimated to be –2.5 ppm using the tabular data given in Emsley, J. W.; Feeney, J.; Sutcliffe, L. H. *High Resolution Nuclear Magnetic Resonance Spectroscopy*; Pergamon Press: Oxford, 1965; Vol. 1, pp 595–604.

## Experimental Section

**1-[2-(1-Naphthyl)phenyl]ethanone (1).** To a stirred solution of palladium tetrakis(triphenyl)phosphine (97 mg, 0.084 mmol) in benzene (20 mL) under nitrogen were added 2-bromoacetophenone (0.42 g, 2.11 mmol), a 2 M NaOH solution (2.2 mL), and 1-naphthyl boronic acid (0.4 g, 2.32 mmol). The reaction mixture was heated at reflux for 12 h and then cooled to room temperature. Aqueous sodium hydroxide (30% w/w) was then added, followed by the slow addition of 30% w/w hydrogen peroxide. The reaction mixture was stirred for 1 h followed by the addition of ether. The layers were separated, and the aqueous layer was further extracted with ether. The combined ether extracts were dried over magnesium sulfate and concentrated under reduced pressure to give the crude product. Flash chromatography on silica gel eluting with ether–hexane (1:9) afforded **1** as a colorless oil (0.41 g, 80%):  $^1\text{H NMR}$  (270 MHz;  $\text{CDCl}_3$ )  $\delta$  1.77 (3H, s,  $\text{CH}_3$ ), 7.31–7.96 (m, ArH);  $^{13}\text{C NMR}$  (67.8 MHz;  $\text{CDCl}_3$ )  $\delta$  29.6 ( $\text{CH}_3$ ), 125.2–141.2 (aromatic signals), 203.0 (C=O); REI-MS  $m/z$  (EI) 246 ( $\text{M}^+$ , 100%), 231 (92), 202 (96), 101 (4) and 84 (8). Anal. Calcd for  $\text{C}_{18}\text{H}_{14}\text{O}$ : C, 87.77; H, 5.73. Found: C, 87.66; H, 5.97. HRMS calcd for  $\text{C}_{18}\text{H}_{14}\text{O}$  246.1045, found 246.1049. This compound has been mentioned but not characterized in a recent communication.<sup>12</sup>

**1-[2-(1-Methylphenyl)ethanone (2).** Palladium tetrakis(triphenyl)phosphine (1.0 g, 0.8 mmol) in benzene (20 mL), 2-bromoacetophenone (4.5 g, 22 mmol), a 2 M NaOH solution (20 mL), and *o*-tolylboronic acid 0.4 g, 2.32 mmol) were combined according to procedures described for the preparation of ketone **1** to give the crude product. Flash chromatography on silica gel eluting with ether–hexane (1:9) afforded **2** as a colorless oil (4.28 g, 81%):  $\nu_{\text{max}}$ (film)/ $\text{cm}^{-1}$  1682 (C=O);  $^1\text{H NMR}$  (270 MHz;  $\text{CDCl}_3$ )  $\delta$  1.98 (3H, s,  $\text{CH}_3$ ), 2.14 (3H, s,  $\text{CH}_3$ ), 7.09–7.69 (m, ArH);  $^{13}\text{C NMR}$  (67.8 MHz;  $\text{CDCl}_3$ )  $\delta$  20.0 ( $\text{CH}_3$ ), 29.6 ( $\text{CH}_3$ ), 125.7–141.8 (aromatic signals), 202.6 (C=O). HRMS calcd for  $\text{C}_{15}\text{H}_{14}\text{O}$  210.1047, found 210.1045. This compound has been recently been reported elsewhere.<sup>13</sup>

**1-Phenyl-2-[2-(1-naphthyl)phenyl]propan-2-ol (3).** A solution of 1-[2-(1-naphthyl)phenyl] ethanone **1** (1.45 g, 5.92 mmol) in dry ether (10 mL) was added dropwise under nitrogen to an ether solution of benzylmagnesium chloride [from magnesium turnings (0.36 g, 15 mmol) and benzyl chloride (2.06 g, 16 mmol) in dry ether (30 mL)]. The reaction mixture was heated at reflux for 12 h and cooled, and a saturated solution of  $\text{NH}_4\text{Cl}$  was added. The aqueous phase was extracted with ether. The organic layer was washed with  $\text{NaHCO}_3$  solution and water, dried over magnesium sulfate, filtered, and concentrated under reduced pressure to give a crude product containing a mixture of two alcohol atropisomers **3a** and **3b** (ratio 1:3 from  $^1\text{H NMR}$  analysis). The crude product was purified by flash chromatography on silica gel eluting with ether–hexane to give alcohol **3a** (0.33 g, 16%) and alcohol **3b** (0.93 g, 46%) both as colorless solids. Compound **3a** was recrystallized from chloroform–hexane, mp 106–107 °C:  $^1\text{H NMR}$  (270 MHz;  $\text{CDCl}_3$ )  $\delta$  1.52 (3H, s,  $\text{CH}_3$ ), 2.82 and 3.13 (each 1H, 2  $\times$  d,  $^2J = 12.8$ ,  $\text{PhCH}_2$ ), 6.19 (1H, dd,  $J = 7.0$ , 1.3, Ar( $2'$ )H), 6.77 (2H, m, *o*-H of  $\text{PhCH}_2$ ), 6.95–7.82 (13H, m, ArH);  $^{13}\text{C NMR}$  (67.7 MHz;  $\text{CDCl}_3$ )  $\delta$  30.62 ( $\text{CH}_3$ ), 75.9 (C-OH), 121.7–145.8 (aromatic signals). Anal. Calcd for  $\text{C}_{25}\text{H}_{22}\text{O}$ : C, 88.72; H, 6.55. Found: C, 88.75; H, 6.33.

Compound **3b** was recrystallized from chloroform–hexane, mp 94–95 °C:  $^1\text{H NMR}$  (270 MHz;  $\text{CDCl}_3$ )  $\delta$  1.09 (3H, s,  $\text{CH}_3$ ); 1.65 (1H, s, OH), 2.94 and 3.14 (1H each, AB system, 2  $\times$  d,  $^2J_{\text{AB}} = 13.5$ ,  $\text{CH}_2$ ), 6.84–7.83 (16H, m, ArH);  $^{13}\text{C NMR}$  (270 MHz;  $\text{CDCl}_3$ )  $\delta$  30.7 ( $\text{CH}_3$ ), 51.3 ( $\text{CH}_2$ ), 77.1 (C-OH), 125.2–146.9 (aromatic signals). Anal. Calcd for  $\text{C}_{25}\text{H}_{22}\text{O}$ : C, 88.72; H, 6.55. Found: C, 88.32; H, 6.56.

## 1-(2-Methylphenyl)-2-[2-(1-naphthyl)phenyl]propan-2-ol (4).

A solution of ketone **1** (2.0 g, 8.1 mmol) in dry diethyl ether (15 mL) was added dropwise under nitrogen to an ether solution of 2-methylbenzylmagnesium bromide [from magnesium turnings (0.48 g, 20.3 mmol) and 2-methylbenzyl bromide (4.13 g, 22 mmol) in dry ether (30 mL)]. The reaction mixture was heated at reflux for 12 h and cooled, and a saturated solution of  $\text{NH}_4\text{Cl}$  was added. The aqueous phase was extracted with ether. The organic layer was washed with aqueous  $\text{NaHCO}_3$  and water, dried over magnesium sulfate, filtered, and concentrated under reduced pressure to give a crude product containing a mixture of two alcohol atropisomers **4a** and **4b** (ratio 1:2 from  $^1\text{H NMR}$  analysis). The crude product was purified by flash chromatography on silica gel eluting with ether–hexane to give alcohol **4a** (0.77 g, 27%) and alcohol **4b** (2.03 g, 71%) both as colorless solids. Compound **4a** was recrystallized from hexane–chloroform, mp 65–66 °C:  $^1\text{H NMR}$  (270 MHz;  $\text{CDCl}_3$ )  $\delta$  1.50 (3H, s,  $\text{CH}_3$ ), 1.56 (1H, br s, OH), 1.83 (3H, s, Ar $\text{CH}_3$ ), 2.92 and 3.04 (each 1H, 2  $\times$  d,  $^2J = 13.4$ ,  $\text{CH}_2$ ), 6.44 (1H, d,  $J = 6.8$ , ArC( $2'$ )H), 6.73 (1H, d,  $J = 7.3$ , *o*-H of *o*-tolyl  $\text{CH}_2$ ), 6.90–7.82 (13H, m, ArH);  $^{13}\text{C NMR}$  (67.8 MHz;  $\text{CDCl}_3$ )  $\delta$  19.7 (Ar $\text{CH}_3$ ), 30.6 ( $\text{CH}_3$ ), 47.1 ( $\text{CH}_2$ ), 76.7 (C-OH), 124.4–146.6 (aromatic signals). Anal. Calcd for  $\text{C}_{26}\text{H}_{24}\text{O}$ : C, 88.60, H, 6.86. Found: C, 88.89, H, 6.95. Compound **4b** was recrystallized from hexane–chloroform, mp 97–98 °C:  $^1\text{H NMR}$  (270 MHz;  $\text{CDCl}_3$ )  $\delta$  1.03 (3H, s,  $\text{CH}_3$ ), 1.66 (1H, s, OH), 1.95 (3H, s, Ar $\text{CH}_3$ ), 3.05 (2H, s,  $\text{CH}_2$ ), 6.85–7.84 (15H, m, ArH);  $^{13}\text{C NMR}$  (67.8 MHz;  $\text{CDCl}_3$ ) 19.9 (Ar $\text{CH}_3$ ), 29.2 ( $\text{CH}_3$ ), 46.3 ( $\text{CH}_2$ ), 76.3 (C-OH), 124.4–150.2 (aromatic signals). Anal. Calcd for  $\text{C}_{26}\text{H}_{24}\text{O}$ : C, 88.60, H, 6.86. Found: C, 88.59; H, 6.86.

## 1-Phenyl-2-[2-(2-methylphenyl)phenyl]propan-2-ol (5).

A solution of 1-[2-(1-methylphenyl)ethanone (**2**) (2.0 g, 9.5 mmol) in dry ether (15 mL) was added dropwise to an ether solution of benzylmagnesium chloride [from magnesium turnings (0.55 g, 23 mmol) and benzyl chloride (3.20 g, 25 mmol) in dry ether (30 mL)] under nitrogen. The reaction mixture was heated at reflux for 12 h and cooled, and a saturated solution of  $\text{NH}_4\text{Cl}$  was added. The aqueous phase was extracted with ether. The organic layer was washed with aqueous  $\text{NaHCO}_3$  and water, dried over magnesium sulfate, filtered, and concentrated under reduced pressure to give a crude product containing a mixture of two alcohol atropisomers **5a** and **5b** (ratio 1:2.7 from  $^1\text{H NMR}$  analysis). The crude product was purified by flash chromatography on silica gel eluting with ether–hexane to give mixed samples of the atropisomers as colorless solids (2.58 g, 92%). Recrystallization of the initial band-head sample from chloroform–hexane afforded compound **5a**, mp 73–74 °C:  $^1\text{H NMR}$  (270 MHz;  $\text{CDCl}_3$ )  $\delta$  1.56 (1H, br s, OH), 1.59 (3H, s,  $\text{CH}_3$ ), 2.03 (3H, s,  $\text{CH}_3$ ), 2.86 and 3.14 (1H each, AB quartet,  $^2J = 13.1$ ,  $\text{CH}_2$ ), 5.89 (1H, d,  $J = 7.3$ , ArC( $6'$ )H), 6.73 [2H, m,  $^3J = 8.2$ , *o*-H of  $\text{PhCH}_2$ ), 6.81–7.64 (m, ArH);  $^{13}\text{C NMR}$  (67.8 MHz;  $\text{CDCl}_3$ )  $\delta$  20.7 (Ar $\text{CH}_3$ ), 30.3 ( $\text{CH}_3$ ), 51.8 ( $\text{CH}_2$ ), 77.0 ( $\text{CH}_2$ –C–OH), 124.7–144.6 (aromatic signals). Anal. Calcd for  $\text{C}_{22}\text{H}_{22}\text{O}$ : C, 87.37; H, 7.33. Found: C, 87.09; H, 7.34. Recrystallization of the band-tail sample gave a pure sample of compound **5b**, mp 67–68 °C:  $^1\text{H NMR}$  (270 MHz;  $\text{CDCl}_3$ )  $\delta$  1.27 (3H, s,  $\text{CH}_3$ ), 1.55 (1H, br s, OH), 1.92 (3H, s,  $\text{CH}_3$ ), 2.98 (1H, d,  $^2J = 13.5$ ,  $\text{CH}_A\text{H}_B$ ), 3.14 (1H, d,  $^2J = 13.5$ ,  $\text{CH}_A\text{H}_B$ ), 6.81–7.64 (m, ArH);  $^{13}\text{C NMR}$  (67.8 MHz;  $\text{CDCl}_3$ )  $\delta$  20.4 (Ar $\text{CH}_3$ ), 29.3 ( $\text{CH}_3$ ), 50.1 ( $\text{CH}_2$ ), 75.8 (C–OH), 124.7–144.6 (aromatic signals). Anal. Calcd for  $\text{C}_{22}\text{H}_{22}\text{O}$ : C, 87.37; H, 7.33. Found: C, 87.57; H, 7.46.

## 1-(2-Methylphenyl)-2-[2-(2-methylphenyl)phenyl]propan-2-ol (6).

A solution of 1-[2-(1-methylphenyl)ethanone (**2**) (2.0 g, 9.5 mmol) in dry ether (15 mL) was added dropwise under nitrogen to an ether solution of 2-methylbenzylmagnesium bromide [from magnesium turnings (0.57 g, 23 mmol) and 2-methylbenzyl bromide (4.57 g, 24.7 mmol) in dry ether (30 mL)]. The reaction mixture was heated at reflux for 12 h and cooled, and a saturated solution of  $\text{NH}_4\text{Cl}$  was added. The aqueous phase was extracted with ether. The organic layer was washed with aqueous  $\text{NaHCO}_3$  and water, dried over magnesium sulfate, filtered, and concentrated under

(12) Tobias, J. K.; Knochel, P. *Angew. Chem. Int. Ed.* **2005**, *44*, 2947–2952.

(13) de Koning, C. B.; Michael, J. P.; Rousseau, A. L. *J. Chem. Soc., Perkin Trans. 1* **2000**, 787–797.

reduced pressure to give a crude product containing a mixture of two alcohol atropisomers **6a** and **6b** (ratio 1:2 from  $^1\text{H}$  NMR analysis). The crude product was purified by flash chromatography on silica gel eluting with ether–hexane to give a sample of mixed isomers (2.12 g, 70%) all as colorless solids. Recrystallization of the initial band-head sample from chloroform–hexane afforded a pure sample of **6a**, mp 60–62 °C:  $^1\text{H}$  NMR (270 MHz;  $\text{CDCl}_3$ )  $\delta$  1.60 (3H, s,  $\text{CH}_3$ ), 1.69 (1H, br s, OH), 1.94 (3H, s,  $\text{CH}_3$ ), 2.02 (3H, s,  $\text{CH}_3$ ), 3.04 (2H, AB quartet,  $^2J = 13.3$ ,  $\text{CH}_2$ ), 6.07 (1H, d,  $J = 7.3$ , ArC(6')H), 6.67 (1H, d,  $J = 7.3$ , *o*-H of *o*-tolyl- $\text{CH}_2$ ), 6.84–7.52 (10H, m, ArH);  $^{13}\text{C}$  NMR (67.8 MHz;  $\text{CDCl}_3$ ) 19.8, (Ar $\text{CH}_3$ ) 20.7 (Ar $\text{CH}_3$ ), 30.5 ( $\text{CH}_3$ ), 47.6 ( $\text{CH}_2$ ), 124.8–144.5 (aromatic signals). Anal. Calcd for  $\text{C}_{23}\text{H}_{24}\text{O}$ : C, 87.30; H, 7.64. Found: C, 87.56; H, 7.68. Atropisomer **6b** could not be obtained completely free of **6a** but a chromatographic fraction highly enriched in **6b** gave the following NMR data: (270 MHz;  $\text{CDCl}_3$ )  $\delta$  1.23 ( $\text{CH}_3$ ), 1.68 (1H, br s, OH), 2.01 (Ar $\text{CH}_3$ ), 2.13 (Ar $\text{CH}_3$ ), 3.06 (2H, m,  $\text{CH}_2$ ), 6.84–7.75 (12H, m, ArH);  $^{13}\text{C}$  NMR (67.8 MHz;  $\text{CDCl}_3$ )  $\delta$  20.9, (Ar $\text{CH}_3$ ) 21.0 (Ar $\text{CH}_3$ ), 29.0 ( $\text{CH}_3$ ), 46.5 ( $\text{CH}_2$ ), 125.1–145.8 (aromatic signals).

**Crystal Data for 3a.**  $\text{C}_{25}\text{H}_{22}\text{O}$ ,  $M_r = 338.4$ , monoclinic,  $a = 10.563(2)$ ,  $b = 9.546(2)$ ,  $c = 19.386(4)$  Å,  $\beta = 105.2(1)^\circ$ ,  $V = 1886.4(11)$  Å $^3$ ,  $T = 293$  K, Cu K $\alpha$  radiation,  $\lambda = 1.54178$  Å, space group  $P2_1/c$ ,  $Z = 4$ ,  $D_x = 1.192$  g cm $^{-3}$ , colorless blocks,  $0.60 \times 0.50 \times 0.50$  mm,  $\mu = 0.54$  mm $^{-1}$ ,  $F(000) = 720$ , Siemens P3/V2000 diffractometer,  $\omega$  scan,  $10^\circ < 2\theta < 110^\circ$ , measured/independent reflections 2509/2355, direct methods solution, full matrix least squares refinement on  $F_o^2$ , anisotropic displacement parameters for non-hydrogen atoms, hydrogens located in difference Fourier but included at positions calculated from the geometry of the molecule using the riding model,  $R1 = 0.046$  for 1760 data with  $F_o > 4\sigma(F_o)$ , 238 parameters,  $wR2 = 0.123$  (all data), goodness of fit = 1.07,  $\Delta\rho_{\text{min,max}} = -0.13/0.15$  e Å $^{-3}$ .

**Crystal Data for 4a.**  $\text{C}_{26}\text{H}_{24}\text{O}$ ,  $M_r = 352.5$ , monoclinic,  $a = 7.526(2)$ ,  $b = 16.602(3)$ ,  $c = 7.809(2)$  Å,  $\beta = 98.9(1)^\circ$ ,  $V = 964.1(3)$  Å $^3$ ,  $T = 293(2)$  K, Cu K $\alpha$  radiation,  $\lambda = 1.54178$  Å, space group  $P2_1$ ,  $Z = 2$ ,  $D_x = 1.214$  g cm $^{-3}$ , colorless blocks,  $0.53 \times 0.47 \times 0.43$  mm,  $\mu = 0.55$  mm $^{-1}$ ,  $F(000) = 376$ , Siemens P3/V2000 diffractometer,  $\omega$  scan,  $10^\circ < 2\theta < 110^\circ$ , measured/independent reflections 1265/1155, direct methods solution, full matrix least squares refinement on  $F_o^2$ , anisotropic displacement

parameters for non-hydrogen atoms; hydrogens located in difference Fourier but included at positions calculated from the geometry of the molecule using the riding model,  $R1 = 0.043$  for 1034 data with  $F_o > 4\sigma(F_o)$ , 248 parameters,  $wR2 = 0.117$  (all data), goodness of fit = 1.06,  $\Delta\rho_{\text{min,max}} = -0.17/0.15$  e Å $^{-3}$ . Although **4a** is racemic the chiral space group  $P2_1$  implies that individual crystals are enantiopure. This was confirmed by recording the CD spectra of a number of randomly selected single crystals, dissolved in acetonitrile. Each crystal was shown to be enantiopure and examples of each enantiomer were identified. Thus the racemic compound was a spontaneously resolved conglomerate comprising RM crystals and SP crystals.

**Variable Temperature NMR and Kinetic Studies.** Variable-temperature NMR spectra were recorded at 270 MHz. Probe temperatures were calibrated using a digital copper–constantan thermometer with the fine sensor inserted into an NMR tube containing 0.6 mL of the appropriate solvent. Proton chemical shifts were referenced to the residual  $\text{CH}_2\text{Cl}_2$  solvent signal set at  $\delta$  5.366 at all temperatures. Atropisomer equilibration experiments were carried out in an NMR tube inserted into a constant-temperature bath. The tube was removed at appropriate time intervals, cooled in ice and the isomer ratio determined by integration of the appropriate methyl signals in the  $^1\text{H}$  NMR spectrum. Rate constants were determined from a standard reversible first-order plot of  $\ln[X_e/(X_e - X)]$  versus temperature affording a slope of  $(k_f + k_r)$ .

**Supporting Information Available:**  $^1\text{H}$  NMR spectra of both atropisomers of compounds **3–6**, graphs of observed and calculated  $^1\text{H}$  chemical shifts versus temperature for the upfield aromatic signal in **3a** and **5a**, and crystallographic details for **3a** and **4a**, including files in CIF format. This material is available free of charge via the Internet at <http://pubs.acs.org>. The CIF files are also available from the Cambridge Crystallographic Data Centre, 12 Union Road, Cambridge, CB2 1EZ, U.K. [fax: +44(0) 1223 336033 or e-mail [deposit@ccdc.cam.ac.uk](mailto:deposit@ccdc.cam.ac.uk)]. CCDC reference numbers 284636 (**3a**) and 284637 (**4a**).

**Acknowledgment.** We thank Dr Paul Stevenson, Queen's University, for helpful discussion relating to the HMBC, HMQC and TOCSY NMR spectra.

JO0520902